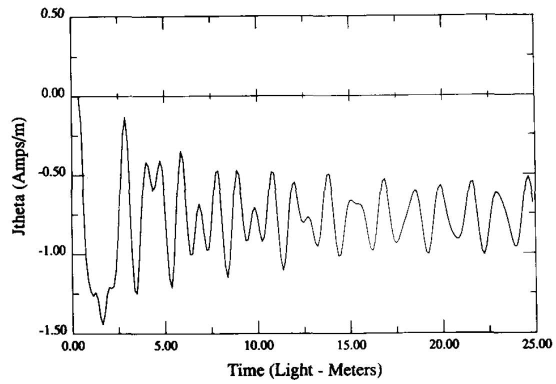

Fig. 4. Transient response at an edge of a hemisphere by a θ-directed current due to an axial step excitation.

For the next example, consider a hemisphere excited by an x-polarized incident electric field applied axially. The hemisphere has a radius of 1 m and the step is incident axially x polarized from the top of the hemisphere. Fig. 4 plots the current J_θ as a function of time at an edge parallel to the rim one third way down from the apex.

V. Conclusion

An alternative version of the time-domain electric field integral equation for arbitrarily shaped conducting structures has been presented. Since this particular time-domain integral equation has one less derivative than conventional methods, impulse and step-like incident waveforms can be considered in this technique. This method is accurate as it provides comparable results to a frequency-domain solution and efficient as Δt may not be dictated by the derivative of the incident field.

References

[1] C. L. Bennett, "A technique for computing approximate electromagnetic impulse response of conducting bodies," Ph.D. thesis, Purdue University, Aug. 1968.
[2] C. L. Bennett and G. F. Ross, "Time domain electromagnetics and its applications," *Proc. IEEE*, vol. 66, pp. 299–318, Mar. 1978.
[3] T. K. Liu and K. K. Mei, "A time domain integral equation for linear antennas and scatterers," *Radio Sci.*, vol. 8, pp. 797–804, 1973.
[4] E. K. Miller, "Direct time domain techniques for transient radiation and scattering from wires," *Proc. IEEE*, vol. 68, pp. 1396–1423, Nov. 1980.
[5] C. L. Bennett and H. Mieras, "Time domain scattering from open thin conducting surfaces," *Radio Sci.*, vol. 16, pp. 1231–1239, Nov.–Dec. 1981.
[6] A. G. Tijhuis, *Electromagnetic Inverse Profiling: Theory and Numerical Implementation.* VNU Science Press, 1987.
[7] B. P. Rynne, "Time domain scattering from arbitrary surfaces using the electric field integral equation," *J. Electromagnetic Waves Appl.*, vol. 5, pp. 93–112, Jan. 1991.
[8] S. M. Rao and D. R. Wilton, "Transient scattering by conducting surfaces of arbitrary shape," *IEEE Trans. Antennas Propagat.*, vol. 39, pp. 56–61, Jan. 1991.
[9] T. K. Sarkar, S. M. Rao, and A. R. Djordjevic, "Electromagnetic scattering and radiation from finite microstrip structures," *IEEE Trans. Microwave Theory Tech.*, vol. 38, pp. 1568–1575, Nov. 1990.
[10] S. M. Rao, T. K. Sarkar, P. Midya, and A. R. Djordjevic, "Electromagnetic scattering from finite conducting and dielectric structures: Surface/surface formulation," *IEEE Trans. Antennas Propagat.*, vol. 39, pp. 1034–1038, July 1991.

Effects of a Resistively Coated Dielectric Strip on the TM-Polarized Resonant Backscatter Behavior of a Slotted Conducting Rectangular Shell

Lin-Kun Wu and Cheng-Hung Lu

Abstract—**The performance of a resistively coated dielectric strip used to suppress the first TM-type resonant backscatter associated with a two-dimensional slotted conducting rectangular shell is analyzed in this paper using the moment method technique. Results obtained indicate that almost perfect resonance damping performances are attained when a finite-dimensioned resistively coated dielectric strip with dielectric constant $\varepsilon_r = 4 - j0.4$ and film resistance $R_s = 188.5\ \Omega$ is placed: (1) at the slot (which directly faces the normally incident TM-polarized plane wave), (2) on the interior perimeter of the shell adjacent to the slot, or (3) at the center of the back wall of the shell. Poorer damping performances are observed, however, when the resistively coated dielectric strip is placed at other positions and/or with the same or higher film resistance. Finally, it is also shown that in general the knowledge of the waveguide theory can be used advantageously in the placement of the resistively coated dielectric strip for achieving best resonance damping performance.**

I. Introduction

The resonant backscatter behavior of cavity-backed apertures in two-dimensional bodies has received much attention recently in connection to its potential importance in the area of target RCS signature [1]–[7]. In general, resonance spikes/nulls found in the RCS spectrum correspond to the resonant modes of the internal (2-D) cavity; the exact relationship between the two depends on the shape and size of the cavity, the location and size of the aperture, and the polarization of the incident wave.

While earlier efforts concentrate on the formulation of solution techniques (e.g., the generalized dual-series approach in [1]–[3] and the moment method solution in [4]–[6]) and investigations of the underlying physics, work described in [7] demonstrates explicitly for the first time the potential use of resistive films for suppressing such resonant RCS behavior. In [7], a special case in which the slot is entirely filled by a resistively coated dielectric strip is analyzed using a finite-difference time-domain method (FD-TD) that incorporates a resistive sheet boundary algorithm for the modeling of resistive films [8]. Although satisfactory numerical results have been obtained with the FD-TD, the severely degraded computational efficiency of the method, due to the use of the resistive boundary algorithm [8], may not be tolerated.

In contrast to [7], an alternative moment method solution procedure is employed in this paper to investigate the ability of a finite-dimensioned resistively coated dielectric strip, when placed at an arbitrary position along the interior perimeter of the slotted shell, to suppress the resonant RCS signature near the first TM resonance region. The cross-sectional geometry of the problem to be attacked is shown in Fig. 1. In the following, a brief summary of the moment method solution procedures is given in Section II. Numerical results showing the effects of the positioning of the resistively coated dielectric strip and film resistance on both the RCS spectrum

Manuscript received August 5, 1992; revised January 13, 1993. This work was supported by the National Science Council of the Republic of China under Grant NSC 81-0404-E-009-545.
The authors are with the Institute of Communication Engineering, National Chiao Tung University, 1001 Ta Hsueh Rd., Hsinchu, Taiwan, Republic of China.
IEEE Log Number 9210817.

0018-926X/93$03.00

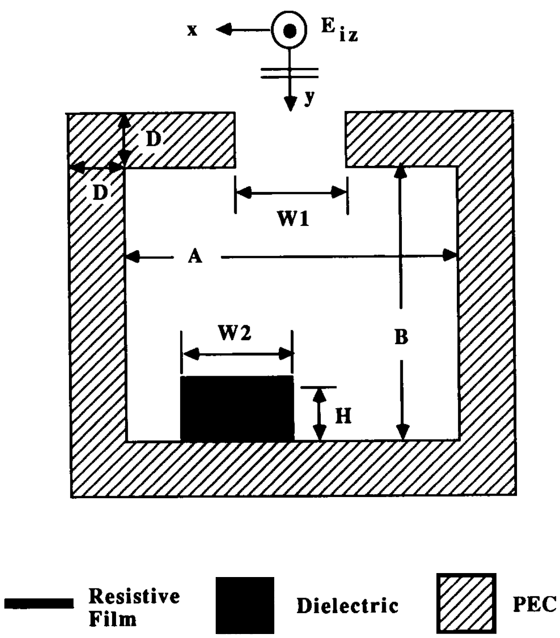

Fig. 1. Geometry of the original two-dimensional problem.

and the interior field distribution are then discussed in Section III. Conclusions are drawn in Section IV.

II. FORMULATION

Consider the problem of a TM-polarized plane wave normally incident on a slotted conducting rectangular shell which is internally loaded by a finite-dimensioned resistively-coated dielectric strip, as shown in Fig. 1. In this analysis, the generally lossy dielectric strip is arbitrarily positioned around the interior perimeter of the shell. The resistive film is assumed to be infinitesimally thin and is characterized by a surface resistance R_s (Ω/square). All materials are assumed to be nonmagnetic with $\mu = \mu_0$, and the composite structure is immersed in free space.

By invoking the equivalence principle [9], the conducting shell and the resistive film can be replaced by z-directed equivalent surface current densities $\boldsymbol{J}_c$ and $\boldsymbol{J}_r$, respectively, and the dielectric strip by the equivalent volumetric polarization current density $\boldsymbol{J}_d$; all of which are situated in free space and are uniform and infinitely long in the z direction. Following the volume/surface formulation of [10], and noting that the tangential (z-directed) electric field induced on the surface of the resistive film (E_{rz}) is related to J_{rz} through the approximate resistive sheet boundary condition [11]

$$E_{rz} = R_s J_{rz}, \tag{1}$$

the following set of coupled electric-field integral equations is obtained:

$$L_1(J_{cz}) + L_1(J_{rz}) + L_2(J_{dz}) = E_{iz}(\boldsymbol{\rho})\text{for } \boldsymbol{\rho} \in C_c \tag{2a}$$

$$L_1(J_{cz}) + L_1(J_{rz}) + L_2(J_{dz}) + R_s J_{rz}(\boldsymbol{\rho}')\delta(\boldsymbol{\rho} - \boldsymbol{\rho}') = E_{iz}(\boldsymbol{\rho})\text{for } \boldsymbol{\rho} \in C_r \tag{2b}$$

$$L_1(J_{cz}) + L_1(J_{rz}) + L_2(J_{dz}) + K_1 J_{dz}(\boldsymbol{\rho}')\delta(\boldsymbol{\rho} - \boldsymbol{\rho}') = E_{iz}(\boldsymbol{\rho})\text{for } \boldsymbol{\rho} \in S_d, \tag{2c}$$

where C_c and C_r denote respectively the perimeter of the conducting shell and resistive film, S_d the cross-sectional area of the dielectric strip, $\boldsymbol{\rho}$ and $\boldsymbol{\rho}'$ the respective position vector to the observer and source, δ the Dirac delta function, $K_1 = -j/\omega\varepsilon_0(\varepsilon_r - 1)$, and $E_{iz}(\rho) = \exp(-jk_0 y)$ for the normally incident, TM-polarized, uniform plane wave. In addition, the two operator equations used in (2) are defined by

$$L_1(J_{qz}) = \frac{\omega\mu_0}{4}\int_{C_q} J_{qz}(\boldsymbol{\rho}')H_0^{(2)}(k_0|\boldsymbol{\rho} - \boldsymbol{\rho}'|)dl' \tag{3a}$$

and

$$L_2(J_{dz}) = \frac{\omega\mu_0}{4}\int\int_{S_d} J_{dz}(\boldsymbol{\rho}')H_0^{(2)}(k_0|\boldsymbol{\rho} - \boldsymbol{\rho}'|)ds', \tag{3b}$$

with k_0 being the free-space wave number, $H_0^{(2)}$ the zeroth-order Hankel function of the second kind, and q stands for either c or r in (3a).

Finally, by subjecting the coupled set of EFIE's given in (2) to the method of moments treatments of subdomain pulse expansion and point-matching testing (which is done at the center of each linear segment/square patch) [12], the following matrix equation is obtained:

$$\begin{bmatrix} [Z_{cc}] & [Z_{cr}] & [Z_{cd}] \\ [Z_{rc}] & [Z_{rr}] & [Z_{rd}] \\ [Z_{dc}] & [Z_{dr}] & [Z_{dd}] \end{bmatrix} \begin{bmatrix} [I_c] \\ [I_r] \\ [I_d] \end{bmatrix} = \begin{bmatrix} [V_c] \\ [V_r] \\ [V_d] \end{bmatrix} \tag{4}$$

The field induced inside the loaded cavity, the far-zone scattered field, and the RCS can then be calculated once the unknown current expansion coefficients (i.e., elements contained in $[I_c]$ $[I_r]$, and $[I_d]$) are obtained by inverting this matrix equation.

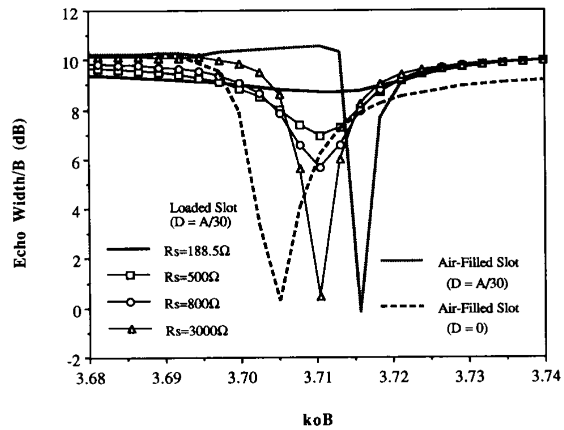

Fig. 2. Echo width spectrum calculated for four loaded slot cases, all with $D = A/30$. Results obtained for the two air-filled slot cases with $D = 0$ and $A/30$ are also shown for comparison.

III. RESULTS ANDDISCUSSION

For the results to be discussed in this section, the following fixed structural parameters are used: $A = 1.5B = 5W1 = 5W2 = 30H$. In addition, the slot is centered on the side of the cylinder facing the incident wave, and $\varepsilon_r = 4 - j0.4$ is used for the dielectric strip. Both zero and finite wall thicknesses are considered. The only variables are then the position of the resistively coated dielectric strip and the film resistance.

A. Loaded Slot

Consider the case in which the slot is entirely filled by a resistively coated dielectric strip with resistive film on the upper side of the strip facing the incident wave. Echo width data obtained for four different film resistances are compared with those of an air-filled slot with $D = 0$ and $A/30$ in Fig. 2. While the TM_{11} mode of a closed

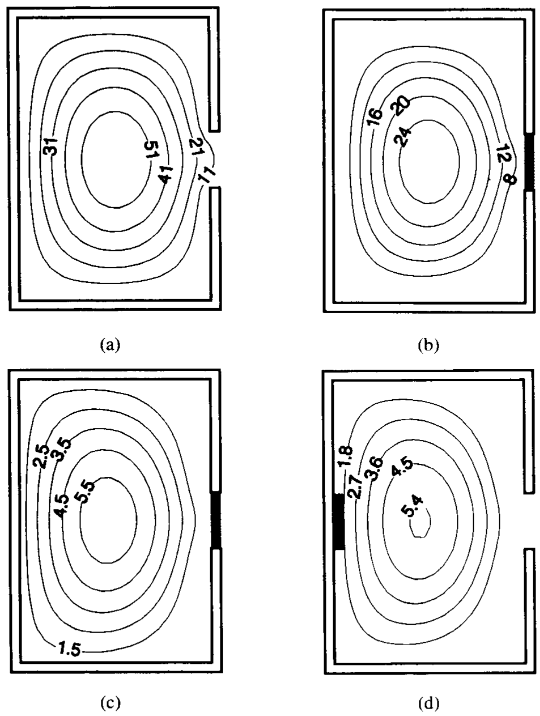

Fig. 3. Contour plots of the electric field induced inside the slotted shell: (a) air-filled slot, (b) loaded slot with $R_s = 3000\ \Omega$, (c) loaded slot with $R_s = 188.5\ \Omega$, and (d) resistively coated dielectric strip with $R_s = 188.5\ \Omega$ is placed at the center of the back wall of the shell. Calculations were made at the corresponding RCS resonance frequency and $D = A/30$.

waveguide with the same A/B ratio as given above cuts off at a normalized frequency of $k_0B = 3.776$, fields coupling across the slot effectively increase the B dimension of the shell, which thus results in lower RCS resonance frequencies for all cases shown in Fig. 2. Furthermore, the slightly higher resonance frequency ($k_0B = 3.716$) found for the air-filled slot with finite depth (compared with $k_0B = 3.705$ found for the air-filled slot with $D = 0$) indicates its ability to "choke" the field that couples across it; this ability is reduced somewhat, however, when the slot is loaded (e.g., it resonates at $k_0B = 3.71$ when $R_s = 3000\ \Omega$).

When the film resistance decreases from 3000 Ω to 188.5 Ω in the loaded slot cases, the depth of the RCS resonance null decreases. In fact, the RCS resonance is almost completely damped when a film resistance of 188.5 Ω is used. To see how this occurs, several plots of the electric field induced inside the cylinder calculated at the frequencies corresponding to their respective RCS null are displayed in Fig. 3. For the air-filled slot case, Fig. 3(a) shows that, except near the slot region, the internal field distribution closely resembles that of the TM_{11} mode for a closed waveguide. Since $|E_{iz}| = 1$ V/m, the induced fields, with peak value > 51 V/m, are very strong. This indicates that a significant portion of the incident power is trapped inside the slotted shell such that a great reduction in the available backscattered power, signified by the deep RCS null shown in Fig. 2, is expected.

Using Fig. 3(a) as a reference, Fig. 3(b) shows a reduction by more than a factor of 2 in the peak induced field for the loaded slot case with $R_s = 3000\ \Omega$. This manifests itself in a slight increase in the corresponding RCS null. By decreasing R_s to 188.5 Ω, the peak induced field is drastically reduced to about 5.5 V/m for the results shown in Fig. 3(c), which also explains the much higher RCS value observed in Fig. 2. For comparison, the field obtained for an additional case in which the resistively coated dielectric strip with $R_s = 188.5\ \Omega$ is placed at the center of the back wall is also shown as Fig. 3(d). In general, field plots shown in parts (c) and (d) of Fig. 3 are quite similar and, although not shown here, similar resonance damping performance is also obtained for this latter loading geometry.

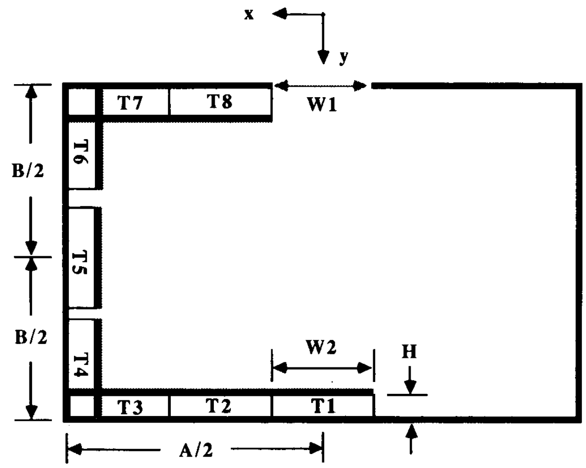

Fig. 4. Specific arrangements of the resistively coated dielectric strip used for the results shown in Fig. 5 ($D = 0$).

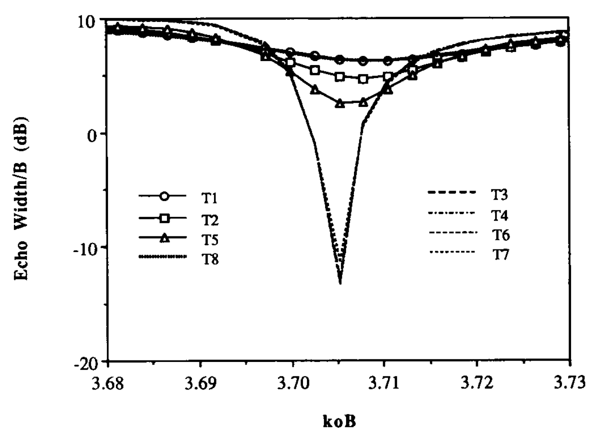

Fig. 5. Echo width data obtained for the problem geometry shown in Fig. 4 with $R_s = 188.5\ \Omega$.

B. Arbitrarily Positioned Resistively Coated Dielectric Strip

Next, we consider the case where the resistively coated dielectric strip is arbitrarily positioned along the interior perimeter of the slotted shell. Zero wall thickness is assumed for simplicity. The arrangement of the eight specific positions used in the numerical computations is shown in Fig. 4, and results obtained for the cases with $R_s = 188.5\ \Omega$ are displayed in Fig. 5.

Fig. 5 shows that the best resonance damping performances are achieved with the resistively coated dielectric strip placed at positions T1, which is centered at the back wall, and T8, which is adjacent to the slot. Since the z-directed current associated with the TM_{11} mode assumes a maximum value at T1 while, with the direction of the induced current parallel to the edge of the slot, extremely large currents are also expected at T8, the excited TM_{11} waveguide mode is highly attenuated by the resistive film in both cases. On the other hand, since zero currents are expected at the corners of an empty waveguide, modal currents at positions T3, T4, T6, and T7 are very small. Resistively coated dielectric strips placed at these locations cannot impose much attenuation on the excited TM_{11} waveguide mode and thus cannot remove the RCS nulls. Finally, although modal currents also peak around position T5, for $A = 1.5B$, they are smaller than the currents induced at T1. Similarly, with the resistively coated dielectric strip displaced from the center of the back wall, smaller modal currents are also expected at T2. These explain their slightly degraded resonance damping performances shown in Fig. 5.

In general, remarks made on the effects of the positioning of the resistively coated dielectric strip for the cases with $R_s = 188.5\ \Omega$ are also applicable to other resistance values and, as seen in Fig. 2, damping performance also degrades in this case as film resistance increases.

IV. Conclusions

The performance of a resistively coated dielectric strip in suppressing the first RCS resonance associated with a slotted conducting rectangular shell is investigated in this paper using the moment method. With the slot centered on the side of the shell facing the normally incident TM-polarized plane wave, almost perfect resonance damping performances are observed when the resistively coated dielectric strip with $R_s = 188.5\ \Omega$ is placed at the slot opening, adjacent to the slot along the interior perimeter of the shell, or at the center of the back wall. However, damping performances are not as good when the resistively coated dielectric strip is placed at other locations and/or with larger film resistances.

In general, the RCS resonance suppression performance achievable by the resistively coated dielectric strip, when affixed at an arbitrary position along the interior perimeter of the slotted shell, is highly correlated to its ability to attenuate the excited TM_{11} modal field. As reported in [1], the specific mode to be excited is dependent upon the positioning of the slot (while the width of the slot affects primarily the bandwidth of the resonance null). It is thus concluded that when the damping of a specific mode is desired, the well-known waveguide theory should be consulted in positioning the resistively coated dielectric strip. This conclusion is expected to be applicable for both rectangular and circular cylindrical shells and for both TM and TE polarizations. However, when the damping of all possible modes across the spectrum is desired, a similar resistively coated dielectric strip that extends over the entire interior perimeter of the slotted shell may be needed. This problem is currently under study, and the results will be reported in the future.

References

[1] W. A. Johnson and R. W. Ziolkowski, "The scattering of an H-polarized plane wave from an axially slotted infinite cylinder: A dual series approach," *Radio Sci.*, vol. 19, pp. 275–291, 1984.

[2] R. W. Ziolkowski, W. A. Johnson, and K. F. Casey, "Applications of Riemann-Hilbert problem techniques to electromagnetic coupling through apertures," *Radio Sci.*, vol. 19, pp. 1425–1431, 1984.

[3] R. W. Ziolkowski and J. B. Grant, "Scattering from cavity-backed apertures: The generalized dual series solution of the concentrically loaded E-pol slit cylinder problem," *IEEE Trans. Antennas Propagat.*, vol. 35, pp. 504–528, May 1987.

[4] T. M. Wang and H. Ling, "Resonant behavior of conducting slotted rectangular shells," *Microwave Opt. Tech. Lett.*, vol. 1, pp. 320–323, Nov. 1988.

[5] T. M. Wang, A. Cuevas, and H. Ling, "RCS of a partially open rectangular box in the resonant region," *IEEE Trans. Antennas Propagat.*, vol. 38, pp. 1498–1504, Sept. 1990.

[6] P. M. Goggans and T. H. Shumpert, "Backscatter RCS for TE and TM excitations of dielectric-filled cavity-backed apertures in two-dimensional bodies," *IEEE Trans. Antennas Propagat.*, vol. 39, pp. 1224–1227, Aug. 1991.

[7] L. K. Wu and L. T. Han, "E-polarized scattering from a conducting rectangular cylinder with an infinite axial slot filled by a resistively coated dielectric strip," *IEEE Trans. Antennas Propagat.*, vol. 40, pp. 731–733, June 1992.

[8] L. K. Wu and L. T. Han, "Implementation and application of resistive sheet boundary condition in the finite-difference time-domain method," *IEEE Trans. Antennas Propagat.*, vol. 40, pp. 628–633, June 1992.

[9] R. F. Harrington, *Time-Harmonic Electromagnetic Fields.* New York: McGraw-Hill, 1961.

[10] T. K. Sarkar and E. Arvas, "Scattering cross section of composite conducting and lossy dielectric bodies," *Proc. IEEE*, vol. 77, pp. 788–795, May 1989.

[11] T. B. A. Senior, "Approximate boundary conditions," *IEEE Trans. Antennas Propagat.*, vol. 29, pp. 826–829, Sept. 1981.

[12] R. F. Harrington, *Field Computation by Moment Method.* New York: Macmillan, 1968.

E-Plane Scan Performance of Infinite Arrays of Dipoles Printed on Protruding Dielectric Substrates: Coplanar Feed Line and E-Plane Metallic Wall Effects

Jean-Pierre R. Bayard, Daniel H. Schaubert, and Michael E. Cooley

***Abstract*—The effects of coplanar feed lines and of E-plane cavity walls on the performance of infinite arrays of dipoles printed on protruding dielectric substrates are investigated. In order to do so, two unit cell configurations are studied: 1) The dipole element fed by coplanar transmission lines and 2) the dipole element fed by coplanar transmission lines with finite-height metallic walls added parallel to the H plane of the array. The element active impedances are calculated for these configurations, and they are compared with those obtained from arrays of dipoles without coplanar feed lines. Effects of the dielectric substrate permittivity and of its thickness on the array element active impedance are included. The results show that the arrays of dipoles with the coplanar feed lines exhibit feed-line-induced blindnesses which reduce considerably the scan volume of the array. It is also shown that these feed line effects are reduced for thicker or higher permittivity substrates, and that the insertion of electric walls is one possible avenue for eliminating these anomalies.**

I. Introduction

In recent years, much attention has been given to phased array analysis and to array elements that can be integrated monolithically with active circuitry. Printed elements on dielectric substrates that protrude from a ground plane are interesting candidates. They are easy to fabricate and the substrate can be extended behind the ground plane for integration of phase shifters, amplifiers, etc. Also, the ground

Manuscript received September 8, 1992; revised January 25, 1993. This work was supported by California State University, Sacramento.

J.-P. R. Bayard is with the Department of Electrical and Electronic Engineering, California State University, Sacramento, CA 95819-6019.

D. H. Schaubert is with the Department of Electrical and Computer Engineering, University of Massachusetts, Amherst, MA 01003.

M. E. Cooley is with Malibu Research Associates, 26670 Agoura Road, Calabasas, CA 91302.

IEEE Log Number 9210866.

0018-926X/93$03.00 © 1993 IEEE